

2023-12

# Anticipatory reward dysfunction in alcohol dependence: An electroencephalography monetary incentive delay task study

Komarnyckyj, M

<https://pearl.plymouth.ac.uk/handle/10026.1/21148>

---

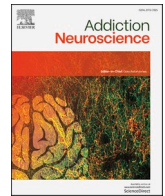
10.1016/j.addicn.2023.100116

Addiction Neuroscience

Elsevier BV

---

*All content in PEARL is protected by copyright law. Author manuscripts are made available in accordance with publisher policies. Please cite only the published version using the details provided on the item record or document. In the absence of an open licence (e.g. Creative Commons), permissions for further reuse of content should be sought from the publisher or author.*



## Anticipatory reward dysfunction in alcohol dependence: An electroencephalography monetary incentive delay task study

Mica Komarnyckyj<sup>a,\*</sup>, Chris Retzler<sup>a</sup>, Robert Whelan<sup>b</sup>, Oliver Young<sup>a</sup>, Elsa Fouragnan<sup>c,d,1</sup>, Anna Murphy<sup>a,\*</sup>

<sup>a</sup> Centre for Cognition and Neuroscience, University of Huddersfield, Queensgate, Huddersfield, HD1 3DH, UK

<sup>b</sup> School of Psychology, Trinity College Dublin, Dublin 2, Ireland

<sup>c</sup> School of Psychology, University of Plymouth, Plymouth, Portland Square, PL4 8AA, UK

<sup>d</sup> Brain Research Imaging Centre, Faculty of Health, University of Plymouth, Plymouth PL6 8BU, UK

### ARTICLE INFO

#### Keywords:

Event-related potentials  
Alcohol dependence  
Reward  
EEG  
Addiction  
Computational psychiatry

### ABSTRACT

A wealth of functional magnetic resonance imaging monetary incentive delay task (MIDT) research has shown alcohol dependency is associated with a hypoactive striatal response during gain anticipation (gain > neutral) and loss anticipation (loss > neutral). Electroencephalography (EEG) holds clinical advantages over fMRI (high temporal resolution, low cost, portable) however its use to study reward processing in alcohol dependence is limited. We aimed to carry out the first EEG MIDT (eMIDT) study in alcohol dependence. 21 abstinent alcohol dependent individuals and 26 controls performed a MIDT while neural activity was recorded using 64-channel EEG. Trial averaged event-related potentials (ERPs) and single-trial machine learning discriminant analyses were applied to EEG data. Clinical variables related to severity of dependence were collected and relationships with ERP data explored. Alcohol dependent individuals, compared with healthy controls, had blunted cue-P3 amplitudes for gain and loss anticipation (interaction:  $p = 0.019$ ); and elevated contingent negative variation amplitudes for all conditions (gain, loss, neutral)(main effect:  $p < 0.001$ ) which was associated with increased alcohol consumption ( $p = 0.002$ ). The machine learning analyses demonstrated alcohol dependent individuals had reduced ability to discriminate between loss and neutral cues between 328 – 350 ms ( $p = 0.040$ ), 354 – 367 ms ( $p = 0.047$ ) and 525 – 572 ms ( $p = 0.022$ ). The eMIDT approach is demonstrated to be a low-cost, sensitive measure of dysfunctional anticipatory reward processing in alcohol dependence, which we propose is ideal for big data approaches to prognostic psychiatry and translation into clinical practice.

### Introduction

Converging research suggests that disruption of the neurobiological networks responsible for reward processing increases vulnerability and supports the maintenance of addiction [1]. The functional magnetic resonance imaging (fMRI) monetary incentive delay task (MIDT) (fMRI-MIDT) has been used extensively to investigate reward function in drug and alcohol dependence. Its strength is the ability to probe both appetitive and consummatory phases of reward processing without excessive demand upon executive function [2,3]. Supporting the 'reward deficiency syndrome' theory of addiction [4], the majority of fMRI-MIDT studies of drug and alcohol dependence report hypoactivation of key reward processing regions, including the ventral

striatum, during both monetary gain and loss anticipation [3,5–8]. Other fMRI-MIDT studies, however, did not replicate these findings, instead reporting comparable striatal sensitivity during anticipatory reward processing in alcohol dependent participants and controls [9–11].

Despite the popularity of the fMRI-MIDT in addiction research, the temporal resolution of the fMRI blood-oxygen-level-dependent (BOLD) signal (in the range of seconds) is not optimal for studying reward-related processing that occurs in the sub-second range [12,13], possibly contributing to inconsistent findings within the fMRI-MIDT literature. In contrast to fMRI, the electroencephalography (EEG) signal is a more direct measure of neural activity, with a temporal resolution in the range of milliseconds, ideal for indexing the range of

\* Corresponding authors.

E-mail addresses: [mica.komarnyckyj@hud.ac.uk](mailto:mica.komarnyckyj@hud.ac.uk) (M. Komarnyckyj), [A.Murphy2@hud.ac.uk](mailto:A.Murphy2@hud.ac.uk) (A. Murphy).

<sup>1</sup> Authors equally contributed to this work.

neural processes that occur during anticipatory and consummatory reward. Disadvantages of EEG include a relatively poor spatial resolution compared with fMRI and issues with detecting signal from deeper brain sources, meaning EEG is unable to precisely measure activity within subcortical reward regions [14]. However, combined EEG-fMRI research suggests EEG is able to probe reward function by detecting cortical downstream consequences of subcortical reward network activation [15]. An additional advantage of EEG is its low setup (£17,000 - £75,000) and running costs [16], whereas fMRI has prohibitive costs (~£2.5 million investment, ~£500/hour rental) which potentially limit study design and present a barrier for translation into clinical practice [17]. The cost effectiveness of EEG is more amenable to widespread clinical use, big data approaches to clinical risk/ treatment response prediction and other ambitious study designs (i.e., large longitudinal studies or neuropharmacological studies investigating multiple drug doses).

EEG versions of the MIDT (eMIDT) have been used successfully to study reward processing in healthy controls (HC), highlighting the cue-P3 event-related potential (ERP) to be an important neurophysiological marker of reward [18–20]. This broad positive wave typically arises between 250 – 600 ms post stimulus onset and is commonly broken down into early cue-P3a and late cue-P3b subcomponents within eMIDT literature [18,21,22]. The cue-P3a and cue-P3b are theorised to reflect stimulus-driven attentional mechanisms and memory/salience processing, respectively [18,23] and have been highlighted as potential clinical markers of alcohol dependence in a recent review article [24].

Research has shown the broad cue-P3 wave (250 – 500 ms) is potentially modulated by central dopamine systems [25]. eMIDT studies with HC demonstrated cue-P3 amplitudes are generally enhanced for monetary gain anticipation [18,20,21,26] and loss anticipation [18,20] and covary with fMRI ventral striatal MIDT response [15]. These findings reflect the ventral striatum BOLD response reported in fMRI-MIDT studies with HC [6–8] and taken together demonstrate the cue-P3 component reliably indexes appetitive neural processing within the reward network.

A further component of interest is the contingent negative variation (CNV), a slow wave related to anticipatory attention and preparation of motivated responses [27,28]. Although, to our knowledge, there are no previous eMIDT studies with substance use disorder or AD participants, our previous eMIDT study with young adult at-risk drinkers showed a trend towards hyperactive CNV salience response (monetary incentive > neutral cues) [21]. A further eMIDT study demonstrated an enhanced CNV salience response (monetary > verbal reward cues) in young adults who had their first drink of alcohol during puberty compared to those who first drank alcohol post-puberty [29].

Here, we carried out the first eMIDT study in alcohol dependence with the aim of investigating anticipatory reward processing with high temporal precision. In addition to traditional ERP analyses, we employed an exploratory whole-brain multivariate linear discriminant machine learning (LD-ML) approach [30,31]. By decoding the experimental conditions across the whole-brain and exploiting information across all electrodes and trials, this method avoids *a priori* electrode choice and achieves improved signal-to-noise ratio (SNR) [32]. Our prior research identified this LD-ML method to have greater sensitivity over traditional ERP methods for detecting reward dysfunction in young-adult at-risk drinkers [21]. We hypothesised AD participants, relative to HC, would exhibit 1) a hypoactive cue-P3 gain and loss anticipatory response [3,5–8,15], 2) a hyperactive CNV salience anticipatory response [21,29], and 3) the magnitude of cue-P3 and CNV would be associated with clinical symptoms of AD (including levels of alcohol consumption and obsessive-compulsive thoughts about alcohol).

## Materials and methods

### Participants

This study included 21 abstinent AD participants (13 male) (mean abstinence duration: 25 months, range: 1 – 130 months; mean age: 45.1 ± 9.3, range: 29 – 60 years) and 26 HC participants (17 male) (mean age: 40.7 ± 10.8, range: 24 – 60 years) (Table 1). We recorded EEG data from 50 participants but excluded 3 due to their failure to complete the task correctly (Supplementary

Methods). Participants were recruited from the University of Huddersfield (UK) campus and local community via flyers, posters, email campaigns, word of mouth, and Facebook groups. AD participants were also recruited from alcohol services in Huddersfield (flyers/posters) and surrounding areas via a targeted Facebook advertising campaign.

All participants had normal or corrected-to-normal vision, normal hearing and were able to read, comprehend and record information in English. AD participants met the DSM-V criteria for severe alcohol use disorder (i.e., score > 6 out of a total score of 11) in their most recent year of drinking alcohol prior to their current period of abstinence (DSM-V mean score: 10.76, score range: 9 - 11), had never met the DSM-V criteria for any other substance use disorder (except nicotine) [33] and were abstinent from alcohol for a minimum of 4 weeks prior to study participation (there was no upper limit for abstinence duration). HC participants had never met the DSM-V criteria for alcohol or drug dependence (except nicotine) [33] and had no first-degree relatives with a history of drug or alcohol dependence. Nicotine dependence was not part of the exclusion criteria for the study. A more detailed description of exclusion criteria is included within the Supplementary Methods.

The study was approved by the University of Huddersfield Department of Applied Sciences Ethics Committee (reference: SAS-SREIC 1.5.19–1).

**Table 1**

Demographic and clinical measures.

	Healthy Control	Alcohol Dependent	p
<b>Demographic variables (mean ± SD)</b>			
Sex (Male/Female)	17/9	13/8	1.000
Age	40.73 ± 10.86	45.10 ± 9.33	0.152
IQ (predicted WAIS based on WTAR)	111.46 ± 4.33	108.04 ± 8.17	0.092
Smoking status (Smoking/Non-Smoking)	11/15	11/10	0.6935
Handedness (EHI > 0 /EHI ≤ 0)	22/4	18/5	0.466
<b>Clinical variables (mean ± SD)</b>			
Age of first alcoholic drink	16.05 ± 3.59	12.33 ± 3.01	< 0.001
Alcohol units per adult year of drinking	968.64 ± 770.19	7409.03 ± 3177.83	< 0.001
AUDIT	4.11 ± 4.07	34.35 ± 3.50	< 0.001
OCDS	1.5 ± 2.75	11.3 ± 9.18	< 0.001
BDI	6.46 ± 5.76	15.45 ± 11.23	0.003
GAD-7	3.31 ± 4.76	5.35 ± 5.54	0.196
CTQ	42.08 ± 11.12	49.50 ± 27.25	0.263
UPPS-NU	22.65 ± 6.87	35.65 ± 7.52	< 0.001
UPPS-PU	19.38 ± 4.67	31.5 ± 10.96	< 0.001

Note: Group differences were evaluated using independent t-tests for continuous variables and Chi-squared test for categorical variables (i.e., sex and smoking status). IQ = Intelligence Quotient; WAIS = Wechsler Adult Intelligence Scale; WTAR = Wechsler Test of Adult Reading; IQ = Intelligence Quotient; EHI = Edinburgh handedness inventory score; AUDIT = Alcohol Use Disorder Identification Test; OCDS = Obsessive Compulsive Drinking Scale; Beck's Depression Inventory = BDI; GAD-7 = Generalised Anxiety Disorder Assessment; CTQ = Childhood Trauma Questionnaire; UPPS-NU = UPPS Negative Urgency; UPPS-PU = UPPS Positive Urgency).

## Experimental sessions

Telephone screening was conducted to verify whether participants met basic eligibility criteria before they were invited to a face-to-face clinical screening which included: written informed consent; alcohol breathalyser and urine drug test (AllTEST™ 10 panel); Mini-International Neuropsychiatric Interview (M.I.N.I.) [34] and DSM-V interview for drug or alcohol dependence; drug and alcohol timeline follow-back interview; Edinburgh Handedness Inventory (EHI) [35]; Wechsler Test of Adult Reading (WTAR) [36]; an online battery of questionnaires (hosted by Qualtrics) which collected demographic and clinical information (Table 1); and 30 practice trials of the eMIDT.

Participants found to be eligible during the clinical screening attended an EEG recording session during which they completed an alcohol breathalyser and urine drug test (AllTEST™ 10 panel), 30 practice trials of the eMIDT and the full eMIDT which consisted of 240 trials. Participants were reimbursed for travel costs and received £10 for attending the clinical screening and £11 - £14 for the EEG recording (depending on eMIDT performance). HC participants could select from Amazon/Sainsbury's vouchers for reimbursement, however, AD participants were given solely Amazon vouchers, since the visibility and accessibility of alcohol in supermarkets may have been problematic.

## Experimental design

Participants performed an EEG version of the MID task (Fig. 1), adapted from that originally used by Knutson with fMRI [2]. A cue symbol was presented for 250 ms which informed participants of the trial type (gain, loss, neutral). A square containing an ascending arrow indicated the potential to win 50p (i.e., gain trials); a square containing a descending arrow indicated the potential to lose 50p (i.e., loss trials); and a square containing a horizontal line indicated there would be no financial outcome (i.e., neutral trials). A white fixation cross was then presented (random jitter of 2000 – 2500 ms) during which participants prepared their motor response for a square target which was presented immediately after.

Participants were instructed to press the space bar as quickly as possible (not more than one time) when the target appeared. A staircase algorithm adapted the target duration to maintain an accuracy of ~66% within each trial type. If accuracy rose above 66% and the participant hit the target, the duration was reduced by 16.67 ms. If accuracy was less than or equal to 66% and the participant missed the target, the duration was increased by 16.67 ms. On all other trials, the target duration

remained unaltered. The algorithm ensured target duration did not fall below 150 ms or go above 350 ms. The starting point for the target duration was informed by the participant's reaction time (RT) on the 30 practice trials.

Following target response, a white fixation cross was presented (random jitter of 1000 – 1200 ms) and participants prepared to view their feedback (shown for 1000 ms). On gain and loss trials participants were shown a tick if they hit the target and a cross if they missed the target, leading to a total of four different outcomes: (1) gain hit trials, a tick was shown and monetary earnings increased by 50 pence; (2) gain miss trials, a cross was shown and monetary earnings stayed the same; (3) loss hit trials, a tick was shown and monetary earnings stayed the same; (4) loss miss, a cross was shown and monetary earnings decreased by 50 pence. Neutral trials had no impact on monetary earnings and no performance feedback was given, instead a horizontal line was shown in place of the tick and cross. Each participant completed 5 blocks of 48 trials each lasting ~4.7 min. The task comprised of 80 win, 80 loss and 80 neutral trials and lasted ~24 min (excluding breaks).

## Experimental stimuli and setup

Our eMIDT task included 3 cue stimuli (Fig. 1) (170 × 141 pixels) which have been validated in prior fMRI-MID task research published by members of our research group [7,37]. Other symbols included a square target (90 × 90 pixels), tick feedback symbol (158 × 98 pixels), cross feedback symbol (157 × 82 pixels) and line feedback symbol (160 × 37 pixels). All symbols were presented in white on a black background. The task was programmed with Psychopy version 1.90.1 [38] (<https://www.psychopy.org/>). It was presented at a frame rate of 60 Hz, using a computer running on Windows 10 (64 bit, 3GB RAM, nVidia GeForce GT 710 graphics card), on a monitor with a resolution of 1920 × 1080 pixels. Participants sat 50 cm from the monitor and responded by pressing the space bar on a USB keypad with the index finger on their dominant hand.

## EEG data acquisition and pre-processing

EEG data were recorded at a sampling rate of 1000 Hz from 64 Ag/AgCl active electrodes, using a 10–20 layout and online reference channel of FCz (ActiCap – Brain Vision, Brain Products, Germany). Channel impedances were kept below 25 kΩ. Pre-processing was performed in EEGLab Toolbox [39] running on Matlab R2019b. Raw data were first downsampled to 500 Hz and high pass filtered at 0.1 Hz to attenuate slow frequency noise. EEG segments where instructions/breaks occurred were removed to improve subsequent channel rejection and independent component analyses (ICA).

The Clean Rawdata EEGLab plug-in (version 2.0) ([https://github.com/sccn/clean\\_rawdata](https://github.com/sccn/clean_rawdata)) was used to reject bad channels (including flat and correlated) which were subsequently interpolated. The Clean-Line EEGLab plug-in (version 1.04) (<https://www.nitrc.org/projects/cleanline>) was used to remove 50 Hz power noise. ICA was employed with principal component analysis enabled to reduce dimensions based on a new data rank, accounting for rank deficiency due to channel rejection and average referencing [40]. The Multiple Artefact Rejection Algorithm (<http://github.com/irenne/MARA>) was used to ensure ICAs were only rejected if there was a high probability (>98%) they represented artefact. The data were low pass filtered at 40 Hz to attenuate high-frequency noise. Finally, the ERPlab plugin [41] (<https://erpinf.org/erplab>) was used to extract cue-locked epochs from the continuous data, with a 500 ms prestimulus and 2000 ms poststimulus period. All epochs were baseline corrected by subtracting the mean voltage of the prestimulus interval between –200 and 0 ms from each epoch, this was done separately for each channel. To conserve as much of the original EEG dataset as possible, epoch rejection was not conducted as part of the pre-processing pipeline. In line with our prior research [31, 42], this maintained trial-by-trial variability which is important for the

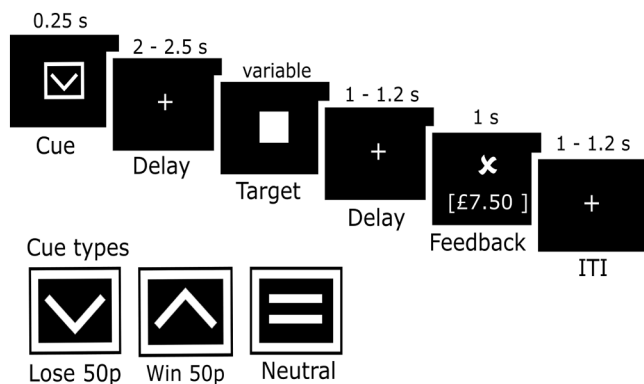


**Fig. 1.** EEG monetary incentive delay task paradigm.

Note: Schematic representation of the eMIDT experimental paradigm. On each trial, one of three cue symbols was presented for 0.25 s indicating if participants could win or lose 50p, or if the trial would have no impact on earnings (i.e., neutral). Following a jittered delay of 2 – 2.5 s a square target was presented. Following a jittered delay of 1 – 1.2 s feedback was shown. A jittered inter-trial interval of 1 – 1.2 s was presented before the next trial began.

LD-ML analyses. Furthermore, it ensured the maximum number of trials were available for the ERP analyses (80 per condition) thus avoiding reduced statistical power which may result from rejecting bad data epochs prior to trial averaging to form ERPs [43]. However, individual subject ERPs were reviewed manually to ensure data cleaning methods had been effective.

#### Event related potential (ERP) analyses

Based on prior eMIDT literature, the cue-P3 was broken down into the cue-P3a and cue-P3b subcomponents, which were quantified over a parietal electrode group (P1, P2, POz, Pz) [21,22,44] and measured as the mean amplitude over 300 – 450 ms and 450 – 600 ms following cue onset, respectively. CNV was measured as the mean amplitude 1800 to 2000 ms post cue onset over a centro-frontal electrode group (C1, C2, FCz, Fz) [21,44].

Mixed model analyses of covariance (ANCOVA) were conducted on mean ERP amplitudes to evaluate group differences. Age, IQ and smoking status were included as covariates based on prior research which has shown these demographic variables can affect the neural response to reward and loss processing [45–47]. The  $3 \times 2$  ANCOVA models used condition (i.e., gain, loss, neutral) as the within-subjects factor and group (i.e., HC group, AD group) as the between-subjects factor. These tests were performed separately for all ERPs (cue-P3a, cue-P3b, CNV).

ERP data entered into the ANCOVA models were checked using Mauchly's Test of Sphericity, if a violation occurred, a Greenhouse-Geisser correction was applied. When ANCOVA tests revealed significant overall results, Tukey post-hoc tests were conducted to investigate which conditions differed significantly from one another. For all statistical tests we used a significance level of  $p < 0.05$ . R software (version 4.0.5) was used for all ERP statistical analyses.

#### Associations between ERP data and clinical severity

For the three time windows of interest (cue-P3a, cue-P3b, CNV), we explored associations between ERP data (ERP difference waves ( $\mu\text{V}$ ): gain-minus-neutral, loss-minus-neutral; and ERP mean amplitude ( $\mu\text{V}$ ): gain, loss) and clinical variables of lifetime alcohol consumption (alcohol units consumed per adult year of active drinking) and Obsessive Compulsive Drinking Scale (OCDS) score (based on an amended version of the OCDS which did not include questions relating to alcohol consumption, see Supplementary Methods) [48], yielding 24 two-way linear regression models (Supplementary Methods). The *p.adjust* function from The R Stats Package [49] was used to apply false discovery rate (FDR) correction for multiple comparisons (24 models). Only models in which ERP data or ERP data by group interaction term was significantly associated with a clinical variable following FDR correction ( $p < 0.05$ ) are included in the results. Diagnostic plots were evaluated from all models and outliers removed (Cook's distance  $> 0.5$ ). This resulted in the removal of a single data point from three regression models.

Within two-way linear regression models, the intercept/constant term refers to the estimated mean Y-value for the reference group, and model coefficients relate to expected changes in mean Y-value relative to this reference [49]. As the present study is focused on identifying reward processing abnormalities associated with alcohol dependency, the AD group was initially specified as the reference group. In models where the ERP data by group interaction term was found to be significant, the linear regression model was rerun specifying HC as the reference group to confirm how the nature of the association differed between groups. R software (version 4.0.5) was used for all regression analyses.

#### Machine learning analyses

We conducted multivariate LD-ML on the single-trial epoched EEG data [21,31]. For each participant, we conducted binary discriminations

across the loss anticipation (loss-vs-neutral) and gain anticipation (gain-vs-neutral) dimensions of reward processing. We estimated a linear weighting contribution (i.e., spatial weighting vector  $w(\tau)$  or spatial filter) for each EEG electrode across the whole brain that gave maximum discrimination between conditions of interest Eq. (1). The LD-ML analyses were conducted across temporally unique training windows, each with a fixed length of  $\delta = 60$  ms and centre times  $\tau$  varying from  $-200$  to  $2000$  ms after cue onset (increasing in increments of 10 ms). A regularised Fisher discriminant estimated  $w(\tau)$  which provided maximum discrimination between electrode signals  $x(t)$  for two conditions (further details are provided in the Supplementary Methods).

$$y_i(\tau) = \frac{1}{N} \sum_{t=\tau-N/2}^{\tau+N/2} w(\tau)^T x_i(t) \quad (1)$$

To evaluate discriminator performance at each training window, we calculated the area under a receiver operating characteristic (ROC) curve ( $A_z$ ) using a leave-one-trial-out (LOTO) cross validation approach randomizing the labels for each trial. The randomisation procedure was repeated 100 times, producing a probability distribution for  $A_z$  and allowing estimation of the  $A_z$  which gave a significance level of  $p < 0.05$ .

We statistically compared group averaged discriminator performance,  $A_z$  values, using SPM1d version 0.4.7 (open-source MATLAB software available from <http://www.spm1d.org/>), as demonstrated in our prior research [21]. SPM1d calculates a scalar trajectory output statistic,  $\text{SPM}\{t\}$ , for individual time nodes across a 1D continuum; where time nodes represented onset times  $\tau$  for the multivariate discriminant analyses and the 1D continuum were pre-hypothesised time windows for components of interest (e.g., cue-P3 and CNV). The  $\text{SPM}\{t\}$  represents only the magnitude of differences between group  $A_z$  values over the 1D continuum, therefore using this scalar trajectory alone will not give conclusive evidence to reject or accept the null hypotheses (i.e., no significant differences in group averaged  $A_z$  values). Random field theory (RFT) was therefore used to define a critical threshold ( $\alpha$ ) that no greater than 5% ( $\alpha < 0.05$ ) of random data that is equally smoothed would be likely to cross. We therefore were able to reject the null hypotheses if  $\text{SPM}\{t\}$  exceeded the critical threshold at any time node [50].

## Results

### Behavioural responses

The mixed model ANCOVA for RT, 3 (condition)  $\times$  2 (group) (age, IQ and smoking status as covariates) showed a significant main effect of condition on RT ( $F(2, 84) = 34.84, p < 0.001, \eta_p^2 = 0.453$ ). Tukey's post-hoc tests revealed that RT for the neutral condition was significantly longer than RT for the gain ( $p < 0.001$ ) and loss ( $p < 0.001$ ) conditions (Table 2). Consistent with prior fMRI-MIDT literature with AD participants [6–8], we found no significant group effects or interactions for RT.

**Table 2**  
Behavioural data.

	Healthy Control	Alcohol Dependent
<b>Reaction time (mean <math>\pm</math> SD)</b>		
Gain (ms)	243 $\pm$ 31	241 $\pm$ 40
Loss (ms)	238 $\pm$ 33	238 $\pm$ 38
Neutral (ms)	269 $\pm$ 35	263 $\pm$ 47
<b>Success rate (mean <math>\pm</math> SD)</b>		
Gain (%)	66 $\pm$ 1.7	66 $\pm$ 1.5
Loss (%)	66 $\pm$ 0.1	66 $\pm$ 1.4
Neutral (%)	65 $\pm$ 5.9	65 $\pm$ 2.3

Note: Reaction time is the time taken by participants to respond to the square target (i.e., time between target onset and keyboard response). The success rate of  $\sim 66\%$  demonstrates the staircase algorithm employed within the task was functioning correctly.

### Effects of alcohol dependency on the cue-P3

For the cue-P3a we found a significant main effect of condition ( $F(2, 84) = 7.25, p = 0.001, \eta_p^2 = 0.148$ ) but no main effect of group ( $F(1, 42) = 0.04, p = 0.826, \eta_p^2 = 0.001$ ) or group by condition interaction ( $F(2, 84) = 0.01, p = 0.991, \eta_p^2 < 0.001$ ). Tukey's post-hoc tests revealed cue-P3a amplitude was significantly larger for the gain condition compared to the neutral condition ( $p = 0.004$ ) (Fig. 2a and b).

For the cue-P3b we found a significant main effect of condition ( $F(2, 84) = 6.47, p = 0.002, \eta_p^2 = 0.134$ ) and a group by condition interaction ( $F(2, 84) = 4.18, p = 0.019, \eta_p^2 = 0.091$ ), but no main effect of group ( $F(1, 42) = 1.16, p = 0.289, \eta_p^2 = 0.027$ ). Tukey's post-hoc tests revealed cue-P3b amplitude was significantly larger for the gain condition compared to the neutral condition ( $p < 0.001$ ) within the HC group but not the AD group (Fig. 2a and b). The HC group displayed a parietal distribution (Fig. 2c) aligned with prior eMIDT literature with controls [20,26], whereas the AD group exhibited a centro-frontal distribution (Fig. 2d). Negative sensor weightings (i.e., blue topography) within the AD group (Fig. 2d) indicate that neural processing for the neutral condition was elevated relative to the gain condition.

### Association between OCDS score and loss-minus-neutral cue-P3a

The model testing for an association between OCDS score, group and loss-minus-neutral cue-P3a difference wave was significant ( $F(3, 42) = 15.05, p_{\text{corr}} < 0.001, R^2 = 0.48$ ). For the AD group, there was a significant negative association between OCDS score and cue-P3a ( $t = -3.43, p_{\text{corr}} = 0.002$ ) (Fig. 2e). The group interaction term was significant ( $t = 2.96, p_{\text{corr}} = 0.005$ ); and the follow-on regression confirmed cue-P3a was not associated with OCDS score in the HC group (Fig. 2e).

### Effects of alcohol dependency on the CNV

We found a significant main effect of condition ( $F(2, 84) = 13.26, p < 0.001, \eta_p^2 = 0.240$ ). Tukey's post-hoc tests revealed CNV amplitude was significantly larger for the gain compared to the neutral condition ( $p <$

0.001) and loss compared to the neutral condition ( $p < 0.001$ ). We also found a main effect of group ( $F(1, 42) = 5.62, p = 0.022, \eta_p^2 = 0.118$ ). Tukey's post-hoc tests revealed CNV amplitude was significantly larger in the AD group compared to the HC group, for the gain ( $p < 0.044$ ), loss ( $p < 0.043$ ), and neutral condition ( $p < 0.016$ ) (Fig. 3a and b). The group by condition interaction was not significant ( $F(2, 84) = 0.48, p = 0.620, \eta_p^2 = 0.011$ ).

### Association between alcohol consumption and CNV

The models testing for an association between alcohol units consumed per adult year of drinking, group, CNV gain ( $F(3, 39) = 43.48, p_{\text{corr}} < 0.001, R^2 = 0.75$ ) and CNV loss ( $F(3, 39) = 15.05, p_{\text{corr}} < 0.001, R^2 = 0.76$ ) were significant. For the AD group, there was a significant negative association between CNV gain ( $t = -3.95, p_{\text{corr}} = 0.008$ ) (Fig. 3c) and CNV loss ( $t = -3.79, p_{\text{corr}} < 0.001$ ) (Fig. 3d). The group interaction terms were significant for both models (CNV gain:  $t = 3.45, p_{\text{corr}} = 0.002$ ; CNV loss:  $t = 3.33, p_{\text{corr}} = 0.002$ ), and follow-on regressions confirmed these ERP components were not associated with alcohol units in the HC group (Fig. 3c and d).

### Effects of alcohol dependency on discrimination between loss and neutral cues

For the HC group, there was a sustained period of significant loss anticipation discrimination (loss-vs-neutral) spanning the entire cue-P3 window (i.e., 300 – 600 ms) (Fig. 4a), whereas the AD group did not exhibit significant loss discrimination following 500 ms (Fig. 4b). At the midpoint of the cue-P3b window (525 ms) the HC group had a parietal distribution which was absent in the AD group (Fig. 4a and b). Within the CNV window, the HC group demonstrated two peaks of significant discrimination (1830 ms, 1932 ms) which were absent in the AD group (Fig. 5a and b).

The SPM1d analyses revealed significant group differences in loss anticipation discrimination within the cue-P3a and cue-P3b window. Significant supra-threshold clusters were found between 328 – 350 ms ( $p_{\text{cluster}} = 0.040, Z = 2.36$ ), 354 – 367 ms ( $p_{\text{cluster}} = 0.047, Z = 2.36$ ) and

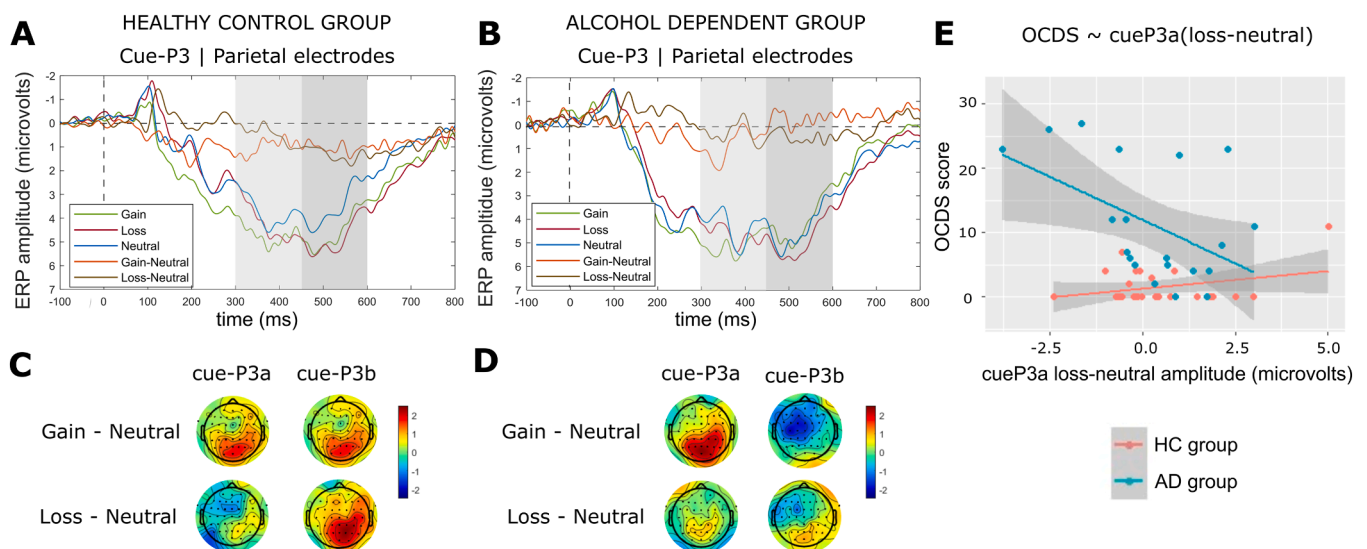


**Fig. 2.** ERP results for the cue-P3a and cue-P3b time windows.

Note: Average cue-P3 ERP components for the HC group (a) and AD group (b), computed over parietal electrodes [P1, P2, POz, Pz]. The first and second grey shaded bars depict the time windows for the cue-P3a and cue-P3b respectively. Scalp topographies are shown for the HC group (c) and AD group (d), for the peaks of the gain-minus-neutral difference wave (315 – 355 ms) and the loss-minus-neutral difference wave (555 – 575 ms) which occurred within the cue-P3 time window (300 – 600 ms). Note that ERPs are plotted with the negative y-axis pointing up. (e) Association between cue-P3a amplitudes (computed for the loss-minus-neutral difference wave over parietal electrodes [P1, P2, POz, Pz]) and OCDS scores. A single data point is included for each HC participant ( $N = 26$ ) and AD participant ( $N = 20$ ) who completed the online clinical questionnaires. The grey shaded region represents a 95% confidence interval for the linear regression lines shown in red (HC group) and blue (AD group).

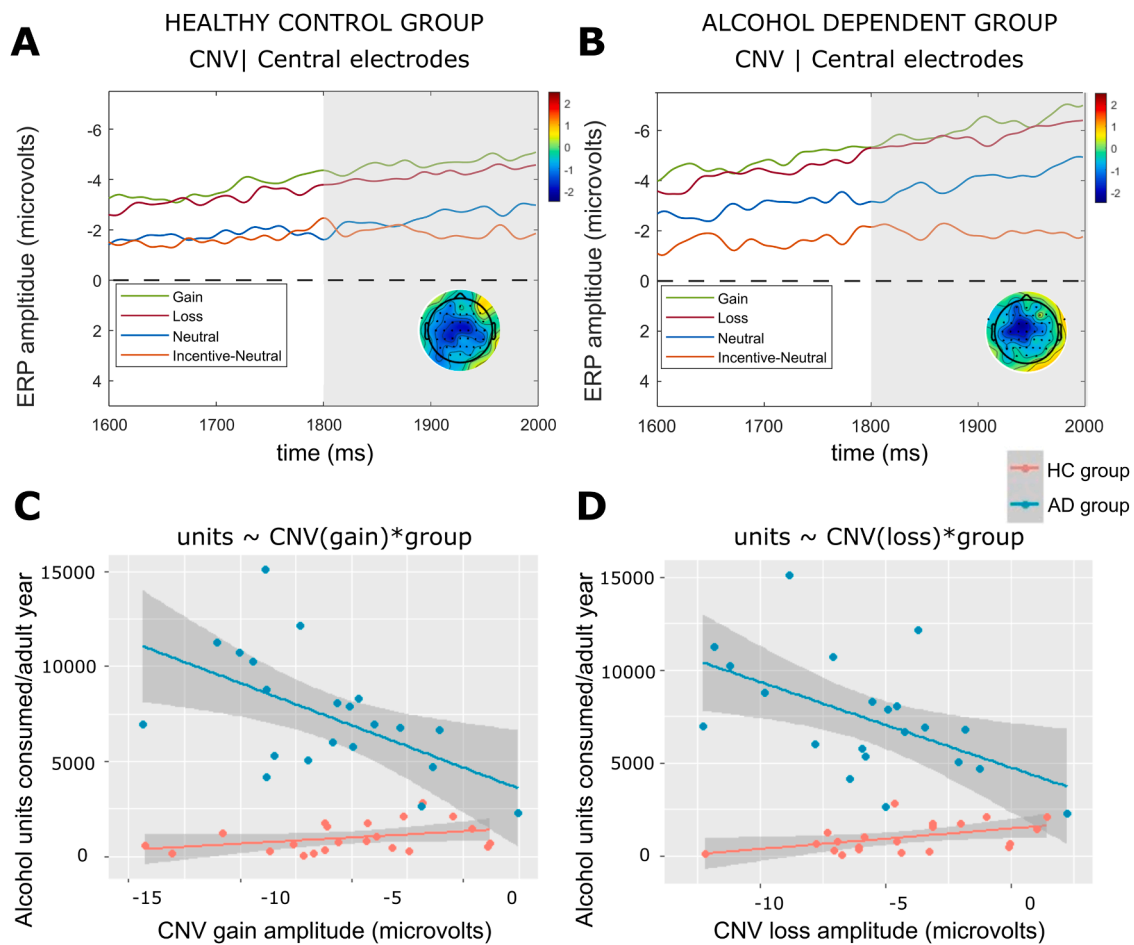


**Fig. 3.** ERP results for the CNV time window.

Note: Average CNV ERP components for the HC group (a) and AD group (b) computed over central electrodes [C1, C2, FCz, Fz]. The grey shaded bars depict the time for the CNV. Scalp topographies are included for peak of the incentive–minus–neutral difference wave (1890 – 1920 ms) which occurred within the CNV time window (1800 – 2000 ms). ERPs are plotted with the negative y-axis pointing up. Regression plots are shown demonstrating the association between (c) gain amplitudes (computed over central electrodes [C1, C2, FCz, Fz]) and alcohol units consumed, and (d) CNV loss amplitudes (computed over central electrodes [C1, C2, FCz, Fz]) and alcohol units consumed. A single data point is included for each HC participant ( $N = 22$ ) and AD participant ( $N = 21$ ) who had consumed alcohol in their lives. The grey shaded region represents a 95% confidence interval for the linear regression lines shown in red (HC group) and blue (AD group).

525 – 572 ms ( $p_{\text{cluster}} = 0.022$ ,  $Z = 2.32$ ). Across suprathreshold time windows,  $A_z$  values for loss anticipation discrimination were significantly larger in the HC group compared to the AD group. We found no significant between group differences in loss vs neutral discrimination within the CNV time window.

#### Effects of alcohol dependency on discrimination between gain and neutral cues

For both the HC and AD groups, we found a broad window of significant gain anticipation discrimination (gain-vs-neutral) spanning the entire window of cue-P3a and cue-P3b (Fig. 4c and d). At the midpoint of the cue-P3b time window (525 ms) the HC group demonstrated a parietal distribution (Fig. 4c). In contrast, the AD group had a centro-frontal distribution with negative sensor weightings (i.e., neural processing for neutral was elevated relative to gain) (Fig. 4d). Within the CNV window, the HC group and AD group exhibited a significant peak of discrimination at 1943 ms and 1830 ms, respectively (Fig. 5c and d). We found no significant between group differences in the magnitude of gain vs neutral discrimination across the cue-P3a, cue-P3b or CNV windows.

## Discussion

### Hypoactive cue-P3b response is evident in alcohol dependency

We aimed to investigate the temporal dynamics of reward dysfunction in alcohol dependency by using an EEG version of the monetary incentive delay task. As hypothesised, we found a hypoactive cue-P3 neural response to gain and loss anticipation vs neutral anticipation in AD compared to control participants. This occurred during the cue-P3b phase and therefore may reflect reduced memory processing of motivationally salient cues in alcohol dependency [18,23]. Whilst this finding of hypoactivation during anticipation of motivationally salient outcomes is consistent with prior fMRI-MIDT literature in substance dependence that also report blunted anticipatory reward processing [5–8] it stands in contrast to other studies which do not report abnormal ventral striatal activity during reward anticipation in alcohol dependent individuals [9–11].

One possible reason for discrepant findings in neural responses during reward anticipation in AD may be MID task design. The large number (240 trials) of fast-paced low-incentive trials in our eMIDT (50 pence at stake for incentive trials, requiring a response every 5 s) may be more sensitive in revealing brain motivational deficits compared with the less demanding shorter fMRI-MIDT paradigms. The latter contained fewer than 100 slow paced trials (~10 - 30 s) with medium (\$1 - \$5

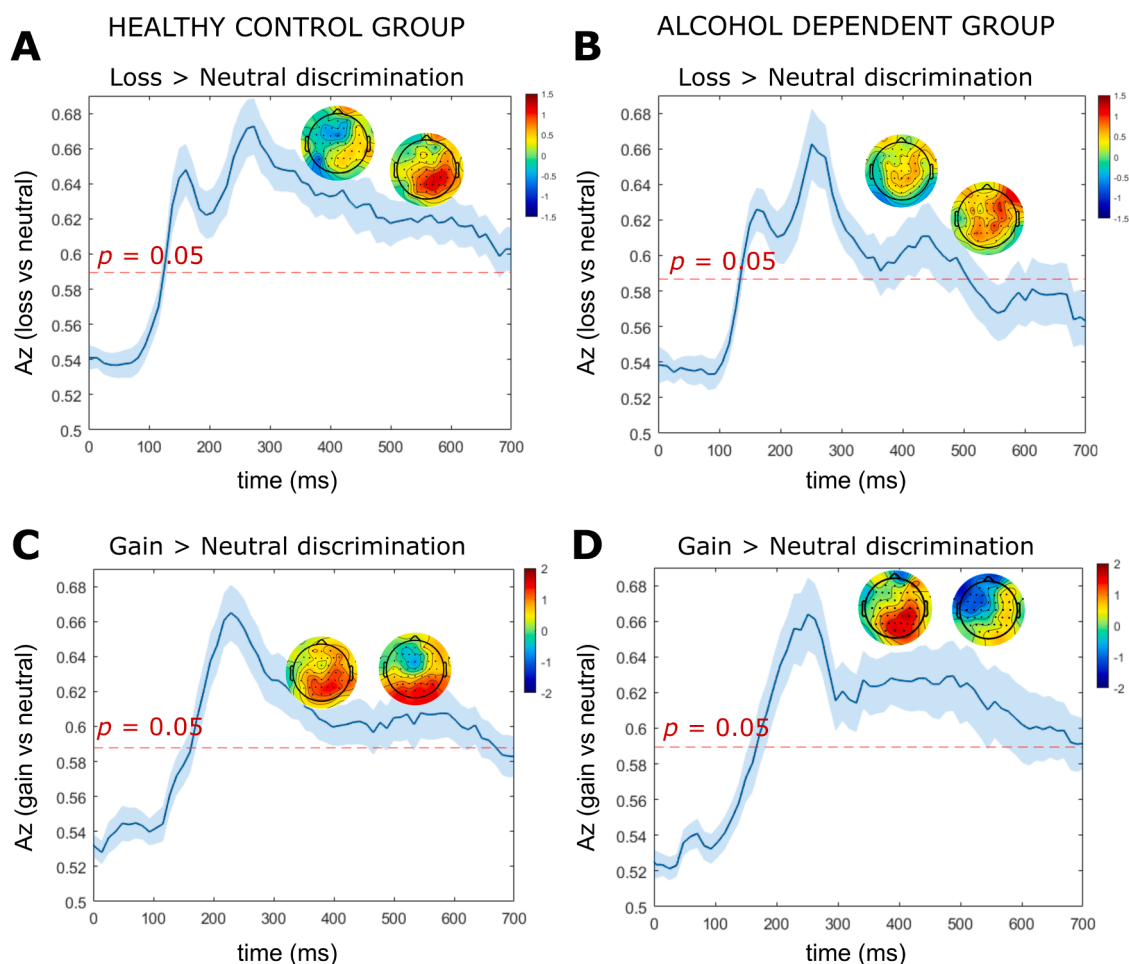


**Fig. 4.** LD-ML results for the cue-P3a and cue-P3b time windows.

Note: Results are averaged over all participants (mean line in blue  $\pm$  se across participants, represented by the shaded blue area). The dotted red line represents the  $A_z$  leading to a significance level of  $p = 0.05$ . The forward models (topographical scalp maps) are presented at the midpoint of the cue-P3a (375 ms) and cue-P3b (525 ms) time windows. (a) Single-trial linear discriminant machine learning (LD-ML) performance ( $A_z$ ) between loss and neutral cues as a function of cue-locked time for the HC group. (b) Single-trial LD-ML performance ( $A_z$ ) between loss and neutral cues as a function of cue-locked time for the AD group. (c) Single-trial LD-ML performance ( $A_z$ ) between gain and neutral cues as a function of cue-locked time for the HC group. (d) Single-trial LD-ML performance ( $A_z$ ) between gain and neutral cues as a function of cue-locked time for the AD group.

stake) [9,10] or high incentives (\$10 stake) [11]. Comparable task performance between HC and AD participants in the current study indicate AD participants were able to perform the eMIDT despite high attentional demands. Although the participants in [9] had a longer mean duration of abstinence than our study (36 months vs 25 months, respectively), similarly we did not find any associations between abstinence duration and neural signal of reward anticipation in exploratory regressions (see Supplementary Results). Taken together these findings suggest that abstinence duration has little effect on the spatial and temporal aspects of the reward processing neural signal in alcohol dependency.

Another possible reason for contradictory findings between our study and prior research in long term abstinence [9] may be modality specific; we propose the high temporal resolution of EEG may be ideal for detecting subtle neural abnormalities that persist into protracted abstinence. In our AD group, it is possible that compensatory neural adaptations occurred to maintain long-term abstinence despite reward deficits. For example, the enhanced CNV response in our sample (discussed later) may have compensated for blunted cue-P3b response to ensure successful task performance. Whilst the millisecond resolution of EEG is ideal for detecting discrete neural events that occur in opposite directions (such as the cue-P3b and CNV), the poor temporal resolution of fMRI may conflate these neural events, preventing their detection.

Our LD-ML results were in agreement with our ERP findings for the cue-P3b. The AD group had significantly reduced LD-ML cue-P3b discriminator performance for loss anticipation (loss-vs-neutral) between 525 – 572 ms. Whilst we did not find group differences in the gain anticipation (gain-vs-neutral) discriminator performance which measures absolute differences in the EEG amplitudes, topographic plots revealed that effects were in opposite directions within each group. For the HC group, discrimination was driven by an enhanced neural response for gain compared to neutral cues, whereas in the AD group, discrimination was driven by enhancement for neutral compared to gain cues. The LD-ML and ERP analyses therefore corroborate one another and support the overall hypothesis that the appetitive cue-P3b response is blunted in AD. We propose this reduced P3b processing is a downstream consequence of dysfunctional ventral striatal processing as found in prior fMRI-MIDT studies in alcohol dependence. The eMIDT cue-P3b is thus highlighted as a neurophysiological marker of dependence, differentiating AD from HC even in protracted abstinence and could have application when investigating novel treatments for addiction.

*Hypoactive cue-P3a loss anticipation is associated with increased OCDS score*

The ERP analyses did not reveal group differences in anticipatory



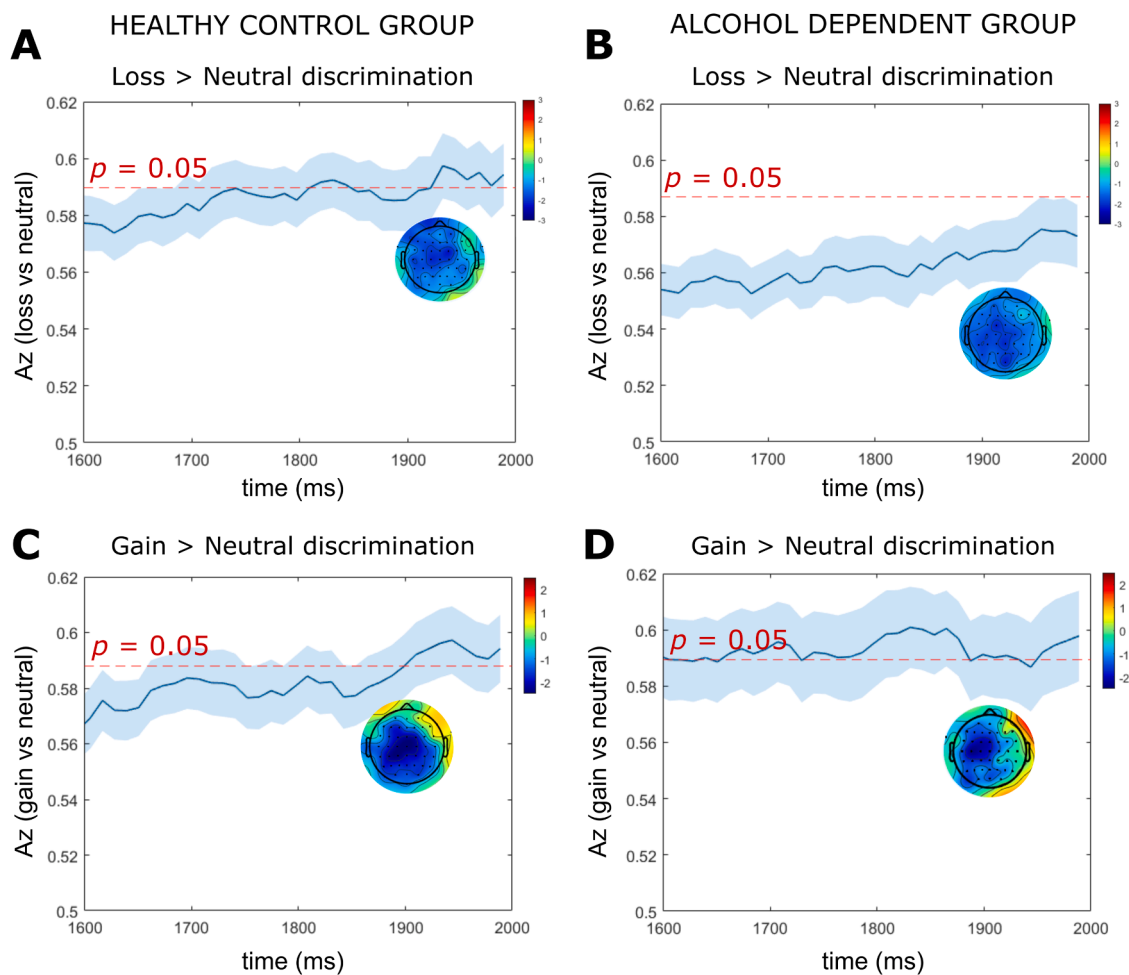


**Fig. 5.** LD-ML results for CNV time window.

Note: Results are averaged over all participants (mean line in blue  $\pm$  se across participants, represented by the shaded blue area). The dotted red line represents the  $A_z$  leading to a significance level of  $p = 0.05$ . The forward models (topographical scalp maps) are presented at the midpoint of the CNV time window (1900 ms). (a) Single-trial linear discriminant machine learning (LD-ML) performance ( $A_z$ ) between loss and neutral cues as a function of cue-locked time for the HC group. (b) Single-trial LD-ML performance ( $A_z$ ) between loss and neutral cues as a function of cue-locked time for the AD group. (c) Single-trial LD-ML performance ( $A_z$ ) between gain and neutral cues as a function of cue-locked time for the HC group. (d) Single-trial LD-ML performance ( $A_z$ ) between gain and neutral cues as a function of cue-locked time for the AD group.

processing for the cue-P3a (300 – 450 ms) whilst the LD-ML analysis did reveal reduced loss vs neutral discrimination in this time period. Inconsistencies between the ERP and LD-ML results may be explained by enhanced SNR offered by the LD-ML approach [21,32] which linearly integrated data from all trials and electrodes across the whole brain rather than averaging data across trials (i.e., ERP). Although the cue-P3a ERP response did not significantly differ from controls when averaging data across the AD group, the regression analysis suggests variation within the group, such that AD participants with increased obsessive-compulsive thoughts about alcohol exhibit blunted cue-P3a loss anticipation. This finding is consistent with a prior fMRI-MIDT study in alcohol dependence that found a similar association between striatal activation and OCDS score [8]. The cue-P3a may therefore represent a neurophysiological marker of persistent vulnerability and relapse risk during protracted abstinence.

#### *Hyperactive CNV is associated with increased alcohol consumption*

During preparation for motor response, we observed a hyperactive CNV signal in alcohol dependence, with amplitudes elevated across all conditions, and greater hyperactivity associated with greater alcohol consumption. Since the AD participants in this study were not actively detoxifying from alcohol (i.e., they were all > 4 weeks abstinence

duration) and exploratory regression analyses (see Supplementary Results) confirmed the CNV signal was not associated with abstinence duration, it is unlikely that this hyperactive CNV signal can be explained by CNS hyperexcitability which occurs during acute alcohol withdrawal [51].

Our results deviate from prior literature reporting reduced CNV amplitudes in dependent active drinkers [52] which may be explained by the differing clinical samples. Our cohort had maintained successful abstinence which relies upon neurobiological changes during the transition from dependence [53]. Despite EEG abnormalities uncovered in alcohol dependency, the groups had comparable RT and success rates. CNV hyperactivity discovered here may therefore indicate a compensatory mechanism, which manifests as more proactive motor inhibition and increased attentional allocation [54,55] in alcohol dependency to achieve the same behavioural eMIDT performance as controls. Potentially, participants who were most severely dependent (i.e., consumed more alcohol) exert greater attentional resources to respond accurately to the eMIDT target (which relies upon successful motor inhibition to prevent premature responses), resulting in the hyperactive CNV signal.

Prior fMRI motor inhibition studies with abstinent drug and alcohol dependent participants also report a hyperactive signal and unimpaired behavioural responses, hypothesised to reflect recovery of cognitive control mechanisms underlying successful abstinence [37,56]. Further

longitudinal research is required to determine whether CNV hyperactivity is a risk marker for high alcohol consumption, or conversely, represents enhanced control mechanisms required to maintain abstinence despite severe dependence.

### Strengths and limitations

Recruitment of an abstinent medication free AD group allowed us to isolate reward dysfunction associated with alcohol dependency and ensure exclusion of the effects of psychoactive substances. This study faced recruitment challenges due to stringent exclusion criteria and covid-19 pandemic lockdowns, which led to a relatively low sample size. There was a wide range in abstinence duration (from 1 month to 130 months) within the AD group which consisted of 21 participants. Notably, the mean abstinence duration was 25 months and most participants (14 out of 21) had been abstinent for 23 months or less. Exploratory analyses (see Supplementary Results) confirmed there were no associations between cue-P3a, cue-P3b or CNV data and duration of abstinence, thus this study cannot make inferences about the impact of protracted vs. short-term abstinence on reward-related EEG measures. The long duration of abstinence within some participants may call into question the reliability of the alcohol consumption measures reported. However, although AD participants had not been actively drinking for months or years, in general they had experience of reporting their alcohol consumption in the time leading up to their abstinence, which is an important and memorable part of the alcohol recovery process, and thus they could easily recall these measures during the clinical assessment process.

Despite these limitations we demonstrated EEG to be a sensitive low-cost approach for detecting reward processing dysfunction in alcohol dependence with both ERP and LD-ML methods. We recommend the clinical utility of the proposed eMIDT risk markers to be validated in large, clinically representative samples (e.g., predict relapse, treatment, progression to alcohol use disorder in ‘at risk’ drinkers). Machine learning analysis of a dataset of hundreds of young adults, including fMRI-MIDT functional markers, personality, cognitive and environmental factors, have been successful at predicting future adolescent alcohol misuse [57]. However, translation into the clinical domain have been limited. It has been argued that much larger training datasets are needed for clinical translatability [58]. Due to the widespread availability, portability, and cost-effectiveness and sensitivity of EEG, we propose the eMIDT to be suitable for future big data approaches to clinical diagnosis and risk prediction.

### Conclusion

Here, we demonstrated eMIDT sensitivity to a hypoactive cue-P3 response to gain and loss anticipation in alcohol dependency, supporting the ‘reward deficiency’ theory of addiction. In contrast, during preparation for motor response we found increased alcohol consumption was associated with a general hyperactive CNV signal in alcohol dependency. The eMIDT markers of alcohol dependency identified here hold potential for big data approaches to clinical diagnosis, prognosis, and clinical translation.

### Author contribution

All authors critically reviewed content and approved the final version for publication.

### CRedit authorship contribution statement

**Mica Komarnyckyj:** Data curation, Investigation, Project administration, Writing – review & editing. **Chris Retzler:** Data curation, Investigation, Formal analysis, Resources, Supervision, Writing – review & editing. **Robert Whelan:** Writing – review & editing. **Oliver Young:**

Data curation, Investigation, Writing – review & editing. **Elsa Fouragnan:** Conceptualization, Methodology, Formal analysis, Resources, Software, Supervision, Writing – original draft, Visualization, Writing – review & editing. **Anna Murphy:** Conceptualization, Methodology, Data curation, Investigation, Resources, Supervision, Writing – original draft, Visualization, Writing – review & editing.

### Declaration of Competing Interest

The authors declare that they have no known competing financial interests or personal relationships that could have appeared to influence the work reported in this paper.

### Acknowledgements

Funding provided by the University of Huddersfield for the PhD studentship that supported MK in this work. EF’s contribution to this work has been funded by a UKRI Future Leader Fellowship Grant (MR/T023007/1). We wish to thank Change Grow Live (CGL) in Huddersfield and the Basement project for promoting the project. The views expressed are those of the author(s) and not those of CGL and associated services. Finally, we wish to thank Ihtisham Ahmed, Katie West, Aisha Lunat and Micheala Marsden for assistance with EEG data collection.

### Supplementary materials

Supplementary material associated with this article can be found, in the online version, at [doi:10.1016/j.addicn.2023.100116](https://doi.org/10.1016/j.addicn.2023.100116).

### References

- [1] G.F. Koob, C.L. Buck, A. Cohen, S. Edwards, P.E. Park, J.E. Schlosburg, et al., Addiction as a stress surfeit disorder, *Neuropharmacology* 76 (2014) 370–382, <https://doi.org/10.1016/J.NEUROPHARM.2013.05.024>.
- [2] B. Knutson, A. Westdorp, E. Kaiser, D. Hommer, FMRI visualization of brain activity during a monetary incentive delay task, *Neuroimage* 12 (2000) 20–27, <https://doi.org/10.1006/nimg.2000.0593>.
- [3] I.M. Balodis, M.N. Potenza, Anticipatory reward processing in addicted populations: a focus on the monetary incentive delay task, *Biol. Psychiatry* 77 (2015) 434–444, <https://doi.org/10.1016/j.biopsych.2014.08.020>.
- [4] K. Blum, E.R. Braverman, J.M. Holder, J.F. Lubar, V.I. Monastra, D. Miller, et al., The reward deficiency syndrome: a biogenetic model for the diagnosis and treatment of impulsive, addictive and compulsive behaviors, *J. Psychoact. Drug.* 32 (2000) 1–112, <https://doi.org/10.1080/02791072.2000.10736099>.
- [5] M. Luijten, A.F. Schellekens, S. Kühn, M.W.J. Machiels, G. Sescousse, Disruption of reward processing in addiction, *JAMA Psychiatry* 74 (2017) 387–398, <https://doi.org/10.1001/jamapsychiatry.2016.3084>.
- [6] A. Beck, F. Schlagenhauf, T. Wüstenberg, J. Hein, T. Kienast, T. Kahnt, et al., Ventral striatal activation during reward anticipation correlates with impulsivity in alcoholics, *Biol. Psychiatry* 66 (2009) 734–742, <https://doi.org/10.1016/J.BIOPSYCH.2009.04.035>.
- [7] L.J. Nestor, A. Murphy, J. McGonigle, C. Orban, L. Reed, E. Taylor, et al., Acute naltrexone does not remediate fronto-striatal disturbances in alcoholic and alcoholic polysubstance-dependent populations during a monetary incentive delay task, *Addict. Biol.* 22 (2017) 1576–1589, <https://doi.org/10.1111/adb.12444>.
- [8] J. Wrase, F. Schlagenhauf, T. Kienast, T. Wüstenberg, F. Bermpohl, T. Kahnt, et al., Dysfunction of reward processing correlates with alcohol craving in detoxified alcoholics, *Neuroimage* 35 (2007) 787–794, <https://doi.org/10.1016/j.neuroimage.2006.11.043>.
- [9] M.P.M. Musial, A. Beck, A. Rosenthal, K. Charlet, P. Bach, F. Kiefer, et al., Reward processing in alcohol-dependent patients and first-degree relatives: functional brain activity during anticipation of monetary gains and losses, *Biol. Psychiatry* 93 (2023) 546–557, <https://doi.org/10.1016/J.BIOPSYCH.2022.05.024>.
- [10] J.M. Bjork, A.R. Smith, D.W. Hommer, Striatal sensitivity to reward deliveries and omissions in substance dependent patients, *Neuroimage* 42 (2008) 1609–1621, <https://doi.org/10.1016/j.neuroimage.2008.06.035>.
- [11] J.M. Bjork, A.R. Smith, G. Chen, D.W. Hommer, Mesolimbic recruitment by nondrug rewards in detoxified alcoholics: effort anticipation, reward anticipation, and reward delivery, *Hum. Brain Mapp.* 33 (2012) 2174–2188, <https://doi.org/10.1002/HBM.21351>.
- [12] W. Schultz, Dopamine neurons and their role in reward mechanisms, *Curr. Opin. Neurobiol.* 7 (1997) 191–197, [https://doi.org/10.1016/S0959-4388\(97\)80007-4](https://doi.org/10.1016/S0959-4388(97)80007-4).
- [13] J.Y. Cohen, S. Haesler, L. Vong, B.B. Lowell, N. Uchida, Neuron-type-specific signals for reward and punishment in the ventral tegmental area, *Nature* 482 (2012) 85–88, <https://doi.org/10.1038/NATURE10754>.

- [14] C.M. Michel, D. Brunet, EEG source imaging: a practical review of the analysis steps, *Front. Neurol.* 10 (2019) 325, <https://doi.org/10.3389/FNEUR.2019.00325/BIBTEX>.
- [15] D.M. Pfabigan, E.-M. Seidel, R. Sladky, A. Hahn, K. Paul, A. Grahl, et al., P300 amplitude variation is related to ventral striatum BOLD response during gain and loss anticipation: an EEG and fMRI experiment, *Neuroimage* 96 (2014) 12–21, <https://doi.org/10.1016/j.neuroimage.2014.03.077>.
- [16] P. Ledwidge, J. Foust, A. Ramsey, Recommendations for developing an EEG laboratory at a primarily undergraduate institution, *J. Undergrad. Neurosci. Educ.* 17 (2018) A10–A19.
- [17] D. Szucs, J.P. Ioannidis, Sample size evolution in neuroimaging research: an evaluation of highly-cited studies (1990–2012) and of latest practices (2017–2018) in high-impact journals, *Neuroimage* 221 (2020), 117164, <https://doi.org/10.1016/J.NEUROIMAGE.2020.117164>.
- [18] D.J. Angus, A.J. Latham, E. Harmon-Jones, M. Deliano, B. Balleine, D. Braddon-Mitchell, Electrocortical components of anticipation and consumption in a monetary incentive delay task, *Psychophysiology* 54 (2017) 1686–1705, <https://doi.org/10.1111/psyp.12913>.
- [19] S.J. Broyd, H.J. Richards, S.K. Helps, G. Chronaki, S. Bamford, E.J.S. Sonuga-Barke, Electrophysiological markers of the motivational salience of delay imposition and escape, *Neuropsychologia* 50 (2012) 965–972, <https://doi.org/10.1016/J.NEUROPSYCHOLOGIA.2012.02.003>.
- [20] G. Chronaki, F. Soltész, N. Benikos, E.J.S. Sonuga-Barke, An electrophysiological investigation of reinforcement effects in attention deficit/hyperactivity disorder: dissociating cue sensitivity from down-stream effects on target engagement and performance, *Dev. Cogn. Neurosci.* 28 (2017) 12–20, <https://doi.org/10.1016/j.dcn.2017.10.003>.
- [21] M. Komarnyckyj, C. Retzler, Z. Cao, G. Ganis, A. Murphy, R. Whelan, et al., At-risk alcohol users have disrupted valence discrimination during reward anticipation, *Addict. Biol.* 27 (2022) e13174, <https://doi.org/10.1111/ADB.13174>.
- [22] A. Vignapiano, A. Mucci, J. Ford, V. Montefusco, G.M. Plescia, P. Bucci, et al., Reward anticipation and trait anhedonia: an electrophysiological investigation in subjects with schizophrenia, *Clin. Neurophysiol.* 127 (2016) 2149–2160, <https://doi.org/10.1016/j.clinph.2016.01.006>.
- [23] J. Polich, Updating P300: an integrative theory of P3a and P3b, *Clin. Neurophysiol.* 118 (2007) 2128–2148, <https://doi.org/10.1016/j.clinph.2007.04.019>.
- [24] R. Jurado-Barba, A. Sion, A. Martínez-Maldonado, I. Domínguez-Centeno, J. Prieto-Montalvo, F. Navarrete, et al., Neuropsychophysiological measures of alcohol dependence: can we use EEG in the clinical assessment? *Front. Psychiatry* 11 (2020) 676, <https://doi.org/10.3389/FPSYT.2020.00676/BIBTEX>.
- [25] O. Pogarell, F. Padberg, S. Karch, F. Segmiller, G. Juckel, C. Mulert, et al., Dopaminergic mechanisms of target detection — P300 event related potential and striatal dopamine, *Psychiatry Res. Neuroimage* 194 (2011) 212–218, <https://doi.org/10.1016/j.psychres.2011.02.002>.
- [26] S.J. Broyd, H.J. Richards, S.K. Helps, G. Chronaki, S. Bamford, E.J.S. Sonuga-Barke, An electrophysiological monetary incentive delay (e-MID) task: a way to decompose the different components of neural response to positive and negative monetary reinforcement, *J. Neurosci. Method.* 209 (2012) 40–49, <https://doi.org/10.1016/j.neumeth.2012.05.015>.
- [27] W.G. Walter, R. Cooper, V.J. Aldridge, W.S. McCallum, A.L. Winter, Contingent negative variation: an electric sign of sensorimotor association and expectancy in the human brain, *Nature* 203 (1964) 380–384, <https://doi.org/10.1038/203380a0>.
- [28] K.D. Novak, D. Foti, Teasing apart the anticipatory and consummatory processing of monetary incentives: an event-related potential study of reward dynamics, *Psychophysiology* 52 (2015) 1470–1482, <https://doi.org/10.1111/psyp.12504>.
- [29] R. Boecker-Schlier, N.E. Holz, E. Hohm, K. Zohsel, D. Blomeyer, A.F. Buchmann, et al., Association between pubertal stage at first drink and neural reward processing in early adulthood, *Addict. Biol.* 22 (2017) 1402–1415, <https://doi.org/10.1111/adb.12413>.
- [30] M.A. Pisauro, E. Fouragnan, C. Retzler, M.G. Philiastides, Neural correlates of evidence accumulation during value-based decisions revealed via simultaneous EEG-fMRI, *Nat. Commun.* 8 (2017) 1–9, <https://doi.org/10.1038/ncomms15808>.
- [31] E. Fouragnan, C. Retzler, K. Mullinger, M.G. Philiastides, Two spatiotemporally distinct value systems shape reward-based learning in the human brain, *Nat. Commun.* 6 (2015) 8107, <https://doi.org/10.1038/ncomms9107>.
- [32] L.C. Parra, C.D. Spence, A.D. Gerson, P. Sajda, Recipes for the linear analysis of EEG, *Neuroimage* 28 (2005) 326–341, <https://doi.org/10.1016/j.neuroimage.2005.05.032>.
- [33] American Psychiatric Association, Diagnostic and statistical manual of mental disorders: substance related and addictive disorders, *Am. Psychiatric Assoc.* (2013), <https://doi.org/10.1176/APPLBOOKS.9780890425596>.
- [34] D. Sheenan, Y. Lecrubier, K. Sheenan, P. Amorim, J. Janavs, E. Weiller, et al., The Mini-International Neuropsychiatric Interview (M.I.N.I.): the development and validation of a structured diagnostic psychiatric interview for DSM-IV and ICD-10, *J. Clin. Psychiatry* 59 (1998) 22–33, <https://pubmed.ncbi.nlm.nih.gov/9881538>.
- [35] R.C. Oldfield, The assessment and analysis of handedness: the Edinburgh inventory, *Neuropsychologia* 9 (1971) 97–113, [https://doi.org/10.1016/0028-3932\(71\)90067-4](https://doi.org/10.1016/0028-3932(71)90067-4).
- [36] D. Wechsler, *Wechsler Test of Adult Reading: WTAR*, 2001.
- [37] A. Murphy, L.J. Nestor, J. McGonigle, L. Paterson, V. Boyapati, K.D. Ersche, et al., Acute D3 antagonist GSK598809 selectively enhances neural response during monetary reward anticipation in drug and alcohol dependence, *Neuropsychopharmacology* 42 (2017) 1049–1057, <https://doi.org/10.1038/npp.2016.289>.
- [38] J. Peirce, J.R. Gray, S. Simpson, M. MacAskill, R. Höchenberger, H. Sogo, et al., PsychoPy2: experiments in behavior made easy, *Behav. Res. Method.* 51 (2019) 195–203, <https://doi.org/10.3758/s13428-018-01193-y>.
- [39] A. Delorme, S. Makeig, EEGLAB: an open source toolbox for analysis of single-trial EEG dynamics including independent component analysis, *J. Neurosci. Method.* 134 (2004) 9–21.
- [40] B.A. Terpou, S.B. Shaw, J. Théberge, V. Férat, C.M. Michel, M.C. McKinnon, et al., Spectral decomposition of EEG microstates in post-traumatic stress disorder, *NeuroImage Clin.* 35 (2022), 103135, <https://doi.org/10.1016/J.NICL.2022.103135>.
- [41] J. Lopez-Calderon, S.J. Luck, ERPLAB: an open-source toolbox for the analysis of event-related potentials, *Front. Hum. Neurosci.* 8 (2014) 213, <https://doi.org/10.3389/fnhum.2014.00213>.
- [42] E. Fouragnan, C. Retzler, M.G. Philiastides, Separate neural representations of prediction error valence and surprise: evidence from an fMRI meta-analysis, *Hum. Brain Mapp.* 39 (2018) 2887–2906, <https://doi.org/10.1002/hbm.24047>.
- [43] A. Delorme, EEG is better left alone, *Sci. Rep.* 131 (13) (2023) 1–12, <https://doi.org/10.1038/s41598-023-27528-0>, 2023.
- [44] Y. Zhang, Q. Li, Z. Wang, X. Liu, Y. Zheng, Temporal dynamics of reward anticipation in the human brain, *Biol. Psychol.* 128 (2017) 89–97, <https://doi.org/10.1016/J.BIOPSYCHO.2017.07.011>.
- [45] D.R. Hawes, C.G. Deyoung, J.R. Gray, A. Rustichini, Intelligence moderates neural responses to monetary reward and punishment, *J. Neurophysiol.* 111 (2014) 1823–1832, <https://doi.org/10.1152/JN.00393.2013>.
- [46] I. Dhingra, S. Zhang, S. Zhornitsky, T.M. Le, W. Wang, H.H. Chao, et al., The effects of age on reward magnitude processing in the monetary incentive delay task, *Neuroimage* 207 (2020), 116368, <https://doi.org/10.1016/J.NEUROIMAGE.2019.116368>.
- [47] J. Peters, U. Bromberg, S. Schneider, S. Brassens, M. Menz, T. Banaschewski, et al., Lower ventral striatal activation during reward anticipation in adolescent smokers, *Am. J. Psychiatry* 168 (2011) 540–549, <https://doi.org/10.1176/APPL.AJP.2010.10071024>.
- [48] R.F. Anton, D.H. Moak, P.K. Latham, The obsessive compulsive drinking scale: a new method of assessing outcome in alcoholism treatment studies, *Arch. Gen. Psychiatry* 53 (1996) 225–231, <https://doi.org/10.1001/ARCHPSYC.1996.01830030047008>.
- [49] R Core Team, R: a language and environment for statistical computing. 2020.
- [50] Pataky T.C., Vanrenterghem J., Robinson M. Statistical Parametric Mapping (SPM): theory, Software and Future Directions. 2017.
- [51] S. Campanella, G. Petit, P. Maura, C. Kornreich, P. Verbanck, X. Noël, Chronic alcoholism: insights from neurophysiology *Alcoolisme chronique et apports de la neurophysiologie*, *Neurophysiol. Clin. Neurophysiol.* 39 (2009) 191–207, <https://doi.org/10.1016/j.neucli.2009.08.002>.
- [52] L.L. Chao, D.J. Meyerhoff, V.A. Cardenas, J.C. Rothlind, M.W. Weiner, Abnormal CNV in chronic heavy drinkers, *Clin. Neurophysiol.* 114 (2003) 2081–2095, [https://doi.org/10.1016/S1388-2457\(03\)00230-X](https://doi.org/10.1016/S1388-2457(03)00230-X).
- [53] H. Garavan, K.L. Brennan, R. Hester, R. Whelan, The Neurobiology of Successful Abstinence, *Curr. Opin. Neurobiol.* 23 (2013) 668–674, <https://doi.org/10.1016/J.CONB.2013.01.029>.
- [54] M. Liebrand, I. Pein, E. Tzvi, U.M. Krämer, Temporal dynamics of proactive and reactive motor inhibition, *Front. Hum. Neurosci.* 11 (204) (2017), <https://doi.org/10.3389/FNHUM.2017.00204/FULL>.
- [55] D. Brevers, G. Cheron, T. Dahman, M. Petieau, E. Palmero-Soler, J. Foucart, et al., Spatiotemporal brain signal associated with high and low levels of proactive motor response inhibition, *Brain Res.* 1747 (2020), 147064, <https://doi.org/10.1016/J.BRAINRES.2020.147064>.
- [56] C.G. Connolly, J.J. Foxe, J. Nierenberg, M. Shpaner, H. Garavan, The neurobiology of cognitive control in successful cocaine abstinence, *Drug Alcohol Depend.* 121 (2012) 45–53, <https://doi.org/10.1016/J.DRUGALCDEP.2011.08.007>.
- [57] R. Whelan, R. Watts, C.A. Orr, R.R. Althoff, E. Artiges, T. Banaschewski, et al., Neuropsychosocial profiles of current and future adolescent alcohol misusers, *Nature* 512 (2014) 185–189, <https://doi.org/10.1038/nature13402>.
- [58] N.K. Dinsdale, E. Bluemke, V. Sundaresan, M. Jenkinson, S.M. Smith, A.I. L. Namburete, Challenges for machine learning in clinical translation of big data imaging studies, *Neuron* (2022) S0896–S6273, <https://doi.org/10.1016/J.NEURON.2022.09.012>.